CrossMark

# Al doped ZnO thin film deposition by thermionic vacuum arc

**Mustafa Özgür[1] · Suat Pat[1] [ORCID] · Reza Mohammadigharehbagh[1] · Caner Musaoğlu[2] · Uğur Demirkol[1] · Saliha Elmas[1] · Soner Özen[3] · Şadan Korkmaz[1]**

## Abstract

ZnO thin films are widely used in many application areas due to its various properties. The properties of the ZnO thin film strongly depend on the manufacturing method, doping elements and ratio and substrate material. In this paper, ZnO material was doped by Al element. Thermionic vacuum arc is a fast deposition technology for Al doped ZnO thin film manufacturing. TVA is physical vapor deposition technology, using anodic vacuum arc. It works under the high vacuum condition. The thin films were deposited onto amorphous glass, semi-crystal PET and single crystal Si substrate. Structural, morphological and optical properties of the Al doped ZnO thin films are presented. Thin films are in polycrystalline form and have high crystalline quality. According to the XRD analysis, metal oxide phases (ZnO and $Al_2O_3$) and bi-metal oxide ($ZnAl_2O_4$) phases were detected. It was found that crystallite sizes strongly depend on the substrate. The crystallite size of the thin film deposited on the Si substrate is approximately 100 nm. For the other sample, the value is very small; it is just about 20 nm. Considering the optical results of the samples, all films are transparent in visible region. Band gap and electronic structures of the Al doped ZnO thin films were investigated by optical method, photoluminescence and Raman spectra. The band gaps of the thin films were shifted towards to the high-energy region. Any impurity in deposited thin films cannot detect by the analyses devices.

## 1 Introduction

ZnO based thin films have gained great interest due to its outstanding properties such as non-toxicity, being abundant in nature, high thermal stability, high transparency and conductivity etc. ZnO has a direct band gap (3.30 eV) [1] with a high exciton binding energy (60 meV) [2] at room temperature. High exciton binding energy makes ZnO an important material for many applications such as UV-lasers [3], solar cells [4], photo detectors [5], LEDs [6] etc. Adjusting the some properties of a thin film is an important prerequisite for many applications. Thus, ZnO thin films should be doped. After the doped ZnO, some properties can change drastically. Al doping element changes to optical band gap of the thin film. Al element is a cheap material. It is non-toxic

material. It is know Al doped ZnO is an alternative material for the transparent conductive oxide layer.

ZnO thin films have been fabricated by several techniques such as chemical vapor deposition [7], pulsed laser deposition [8], chemical bath deposition [9], sol–gel [10] and thermionic vacuum arc (TVA) [11] deposition technique.

In this study TVA deposition has been used for fabrication of the Al doped ZnO thin films. TVA is a unique deposition technique among the others. Thin films produced by TVA deposition technique are extremely flat, having low roughness, nano structured, transparent, as reported earlier [12–14]. In this study, Al doped ZnO thin films has been produced onto glass, polyethylene terephthalate (PET) and silicon (Si) substrate. Morphological, structural and optical properties and substrate effect of the Al doped ZnO thin films have been investigated. ZnO and ZnO semiconductors show magnetic and photocatalytic properties [15], optical properties [16] electronic properties [17], transparent conductive oxide [18], etc. have been widely studied around the world. However, it is a still an attractive material to be studied.

✉ Suat Pat
 suatpat@ogu.edu.tr

1 Department of Physics, Eskişehir Osmangazi University, Eskisehir, Turkey

2 Department of Nanoscience and Nanotechnology, Eskişehir Osmangazi University, Eskisehir, Turkey

3 Department of Occupational Health and Safety, Bozok University, Akdağmadeni, Yozgat, Turkey

## 2 Experimental setup

TVA deposition technique is an anodic plasma generator and it works under the high vacuum condition. It is a good technique to produce high purity, nano structured, thin films with less roughness. In principle, TVA experimental system consists of anode, which represents tungsten crucible with spoon-like shape, and cathode, which represents electron gun (tungsten filament). The anode material is located inside the crucible and both electrodes are located inside the vacuum chamber. The cathode is a coil with four-turn, made of tungsten wire with a thickness of 0.4 mm and 1 mm inner radius. Experimental setup of the TVA system is shown in Fig. 1. As seen in figure AC voltage applied to the tungsten filament. As a result, cathode emits thermal electrons. Emitted electrons are collimated via Wehnelt cylinder and are accelerated towards the anode under the high DC voltage. When accelerated electrons reach the anode from the heated cathode, a continuous evaporation of the anode material is established. With a further increase of the applied voltage, a bright discharge is established between the electrodes. Finally, deposition will take place when the energetic ions in the plasma of the coating material reach the substrate.

TVA deposition is a very promising and relatively a new method for fabrication of the thin films. The advantages of this method, ion energies can be controlled even during the experiment. In addition to it does not require any buffer or mixture gas thus it provides to produce thin films by keeping impurity level at the minimum. Furthermore, it can provide fabrication of the multiple thin films even with the different coating materials simultaneously [18, 19].
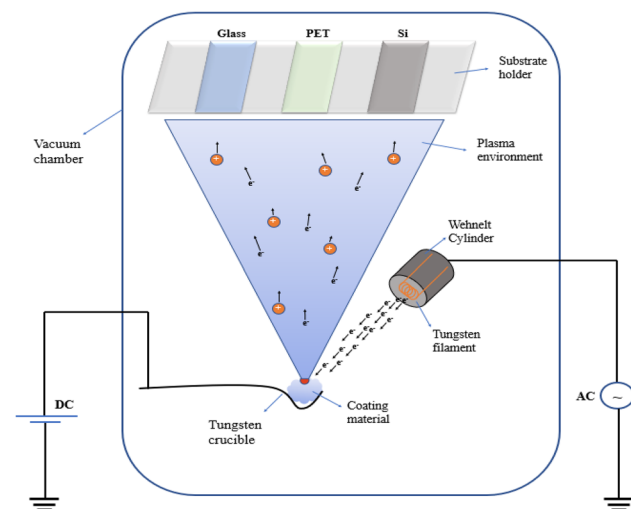
All doping Al and ZnO material were in powder form with purity of 99.99%. Materials prepared in disk shape by using high-pressure pellet machine before the deposition process. The material to be evaporated consists of ZnO:Al disk with 3 mm diameter and 1 mm thickness. The used substrates were prepared by using ultrasonic bath apparatus for 20 min for several times and then cleaned with ethyl alcohol before adjusting on the substrate holder. Deposition was performed under the high vacuum (from $7 \times 10^{-5}$ to $2 \times 10^{-4}$ torr) conditions. The applied voltage between the electrodes decreased from 1500 to 400 V and the deposition performed last 1 min. The ignition of the plasma causes a decrease of the chamber pressure and the applied voltage whereas the discharge current occurs (from 0 to 0.4 A). The experimental parameters also summarized in Table 1.

## 3 Results and discussion

In this study Al doped ZnO thin films were fabricated make use of the TVA technique onto amorphous glass, polycrystalline PET and single crystal Si (111) substrate. The morphological, structural and optical properties of the samples have been investigated with various analysis devices.

Considering the XRD results, all fabricated films are in polycrystalline form and are show different crystalline orientation in terms of substrate effect. The measurement was taken place in the range of 20°–80° and results are shown in Fig. 2. $ZnAl_2O_4$ bi-metal oxide has been found for all substrate in cubic form and matched with crystallographic database number 96-900-7033 for Match software and literature [20]. $ZnAl_2O_4$ is a spinel type oxide and is known to have high chemical and thermal stability, high mechanical resistance and low surface acidity all of which make it a suitable material for a wide range of applications [21]. Aluminum oxide ($Al_2O_3$) peak that correspond to highest peak in XRD pattern was found in orthorhombic space group and obtained results show a good associated with Match software crystallographic database number 96-810-3789 and literature [22]. The other constructive interference peak of



**Fig. 1** Illustration of experimental setup of the thermionic vacuum arc system

**Table 1** Experimental parameters of the AZO thin films deposition

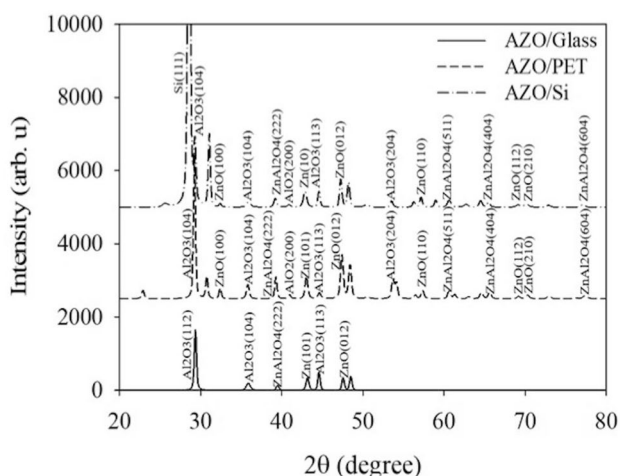| Experimental parameters | Value |
| --- | --- |
| Working pressure | $7 \times 10^{-5}$ – $2 \times 10^{-4}$ torr |
| Filament current | 20 A |
| Applied voltage | 1500 V |
| Discharge current | 0.4 A |
| Deposition time | 60 s |

**Fig. 2** XRD pattern of the deposited AZO thin films onto glass, PET and Si

the Al, ZnO, $AlO_2$ and $Al_2O_3$ was found in the XRD pattern at various degrees. The XRD peaks are also associated with the literature [23–27].

The surface morphology, were determined by using an Ambios Q-Scope atomic force microscope (AFM) in non-contact mode. The measurement was taken place in the range of 4 µm × 4 µm as seen in Fig. 3. The AFM images

of the samples showed granular film structure with spherical grains of varying sizes.

The crystallite sizes were calculated by Scherrer equation [28, 29];

$$D = \frac{k\lambda}{\beta\cos\theta} \tag{1}$$

where $D$ is the crystallite size, $K$ is a shape factor which is selected a 0.94, $\lambda$ is used wavelength in XRD measurement, $\beta$ is a full width at half maximum (FWHM) value of the respective diffraction peak, $\theta$ represents the peak position. Crystallite size values were obtained between ~20 nm and ~100 nm for three different substrates. Dislocation density ($\delta$) and internal strain ($\varepsilon$) were calculated by the following equations:

$$\delta = \frac{1}{D^2} \tag{2}$$

$$\varepsilon = \frac{\beta\cos\theta}{4} \tag{3}$$

The obtained results are summarized in Table 2. Obtained results show that the crystallite size values relatively higher for Si substrate compared to PET and glass substrate. It can be concluded that nano-crystallites can be
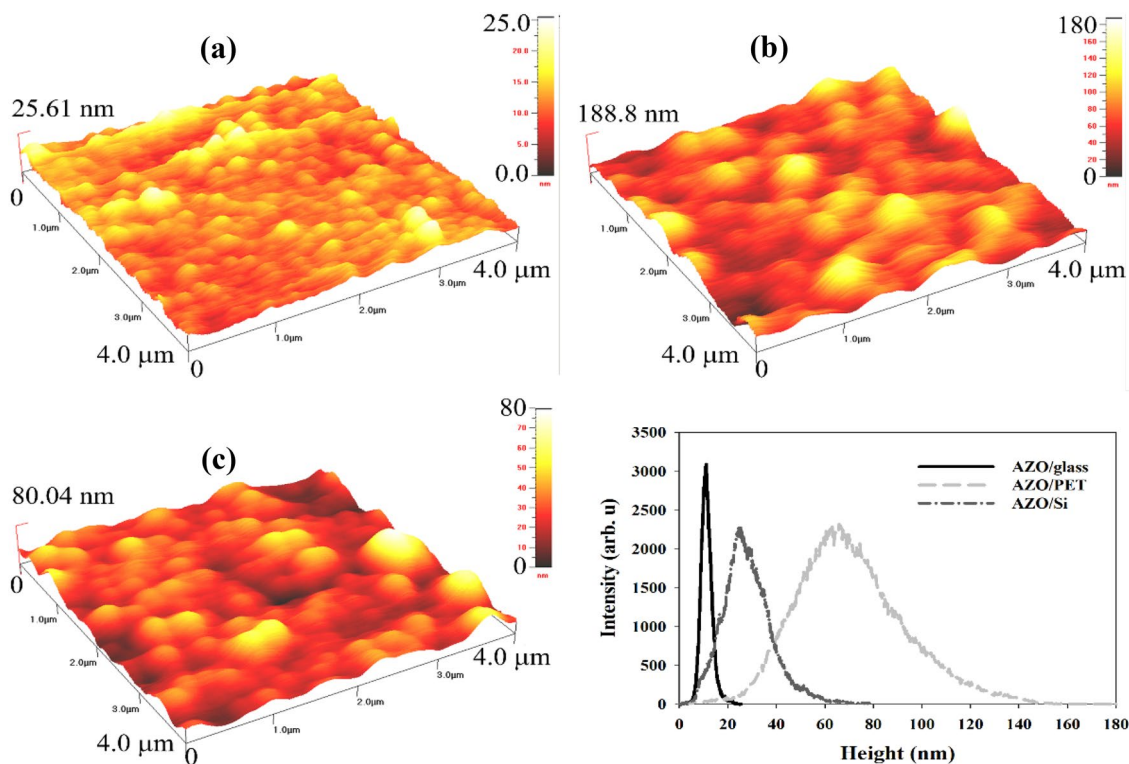


**Fig. 3** AFM images and height distribution of the AZO thin films deposited onto **a** glass, **b** PET, and **c** Si substrate

**Table 2** XRD patterns, peak positions and calculated crystallite sizes, dislocation density, micro strain values

|  | 2θ (Degrees) | Diffraction plane | Miller indices | D (nm) | $\varepsilon \times 10^{-3}$ | $\delta$ ($\times 10^{-3}$ nm$^{-2}$) |
|---|---|---|---|---|---|---|
| Onto glass substrate | 29.32 | $Al_2O_3$ | (112) | 26 | 5.45 | 1.45 |
|  | 35.86 | $Al_2O_3$ | (104) | 15 | 7.67 | 4.26 |
|  | 39.45 | $ZnAl_2O_4$ | (222) | 20 | 5.27 | 2.41 |
|  | 43.13 | Zn | (101) | 20 | 4.72 | 2.30 |
|  | 44.60 | $Al_2O_3$ | (113) | 27 | 3.52 | 1.36 |
|  | 47.55 | ZnO | (012) | 25 | 3.53 | 1.54 |
| Onto PET substrate | 29.21 | $Al_2O_3$ | (112) | 28 | 1.27 | 5.11 |
|  | 32.38 | ZnO | (100) | 27 | 1.34 | 4.75 |
|  | 35.78 | $Al_2O_3$ | (104) | 20 | 2.30 | 5.65 |
|  | 39.23 | $ZnAl_2O_4$ | (222) | 26 | 1.38 | 4.00 |
|  | 40.93 | $AlO_2$ | (200) | 48 | 0.43 | 2.15 |
|  | 42.99 | Zn | (101) | 21 | 2.14 | 4.57 |
|  | 44.59 | $Al_2O_3$ | (113) | 24 | 1.68 | 3.92 |
|  | 47.38 | ZnO | (012) | 21 | 2.15 | 4.17 |
|  | 53.67 | $Al_2O_3$ | (204) | 24 | 1.74 | 3.34 |
|  | 57.30 | ZnO | (110) | 21 | 2.18 | 3.52 |
|  | 60.57 | $ZnAl_2O_4$ | (511) | 20 | 2.33 | 3.46 |
|  | 65.57 | $ZnAl_2O_4$ | (404) | 21 | 2.09 | 3.06 |
|  | 69.12 | ZnO | (112) | 109 | 0.08 | 0.58 |
|  | 70.26 | ZnO | (201) | 55 | 0.33 | 1.14 |
|  | 77.31 | $ZnAl_2O_4$ | (602) | 115 | 0.07 | 0.50 |
| Onto Si substrate | 29.26 | $Al_2O_3$ | (112) | 20 | 2.36 | 6.95 |
|  | 32.38 | ZnO | (100) | 93 | 0.11 | 1.38 |
|  | 35.88 | $Al_2O_3$ | (104) | 94 | 0.11 | 1.24 |
|  | 39.16 | $ZnAl_2O_4$ | (222) | 95 | 0.11 | 1.13 |
|  | 40.83 | $AlO_2$ | (200) | 96 | 0.11 | 1.08 |
|  | 42.83 | Zn | (101) | 48 | 0.43 | 2.05 |
|  | 44.54 | $Al_2O_3$ | (113) | 49 | 0.41 | 1.92 |
|  | 47.24 | ZnO | (012) | 25 | 1.48 | 3.48 |
|  | 53.50 | $Al_2O_3$ | (204) | 101 | 0.10 | 0.80 |
|  | 57.14 | ZnO | (110) | 102 | 0.09 | 0.74 |
|  | 60.59 | $ZnAl_2O_4$ | (511) | 104 | 0.09 | 0.69 |
|  | 65.45 | $ZnAl_2O_4$ | (404) | 107 | 0.09 | 0.62 |
|  | 69.08 | ZnO | (112) | 109 | 0.08 | 0.58 |
|  | 70.08 | ZnO | (201) | 110 | 0.08 | 0.57 |
|  | 77.00 | $ZnAl_2O_4$ | (602) | 115 | 0.08 | 0.50 |

grown with lower size onto amorphous substrates rather than crystal substrates.

The FESEM measurements were taken in order to investigate surface topography of the samples using Carl Zeiss Supra VP40 FESEM device. The measurement results are shown in Fig. 4 with 100k times magnification. As seen in figure, the deposited film onto the glass substrate has lower grain size compared to grain size of the PET and Si substrate. The FESEM results are in good agreement with the AFM measurements.

The optical analysis of the Al doped ZnO thin films were conducted by using UV–Visible spectrophotometry and Filmetrics F20 thin film thickness measurement system. Transmittance values of the thin films were obtained as ~ 50% and ~ 30% in visible spectrum for glass and PET substrate respectively. Reflectance, refractive index and extinction coefficient data are also shown in Fig. 5. Cauchy dispersion model, was used in order to obtain the refractive index n(λ) as a function of the wavelength. Cauchy model is given by:

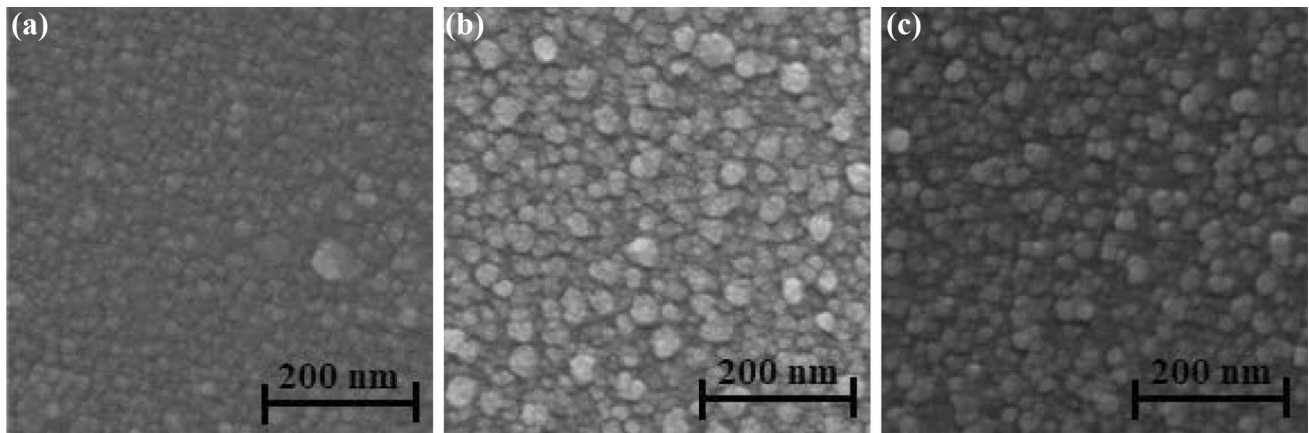$$n(\lambda) = A_n + \frac{B_n}{\lambda^2} + \frac{C_n}{\lambda^4} + \cdots \tag{4}$$

**Fig. 4** FESEM images of the AZO thin films deposited onto **a** glass, **b** PET, and **c** Si substrate
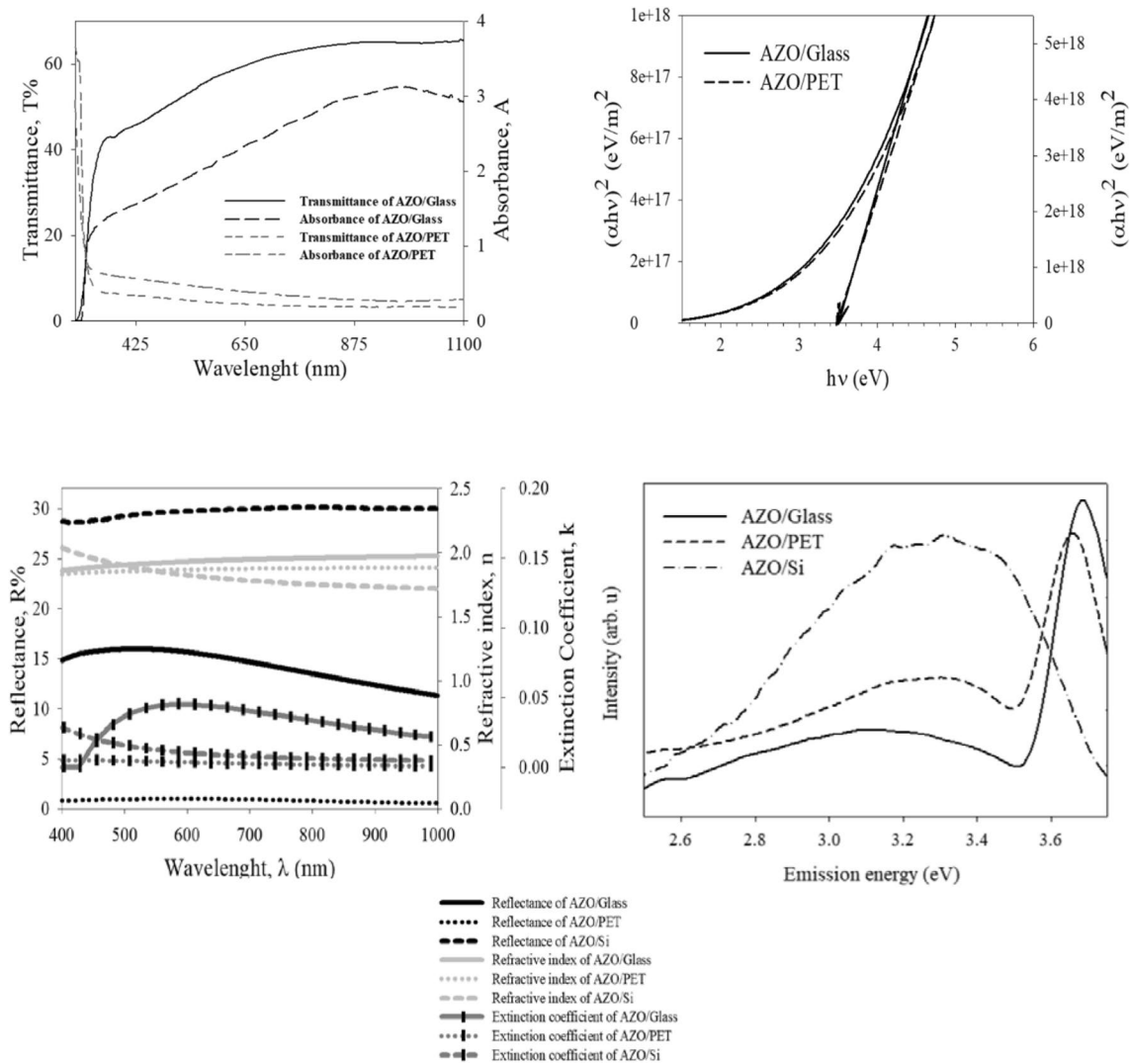


**Fig. 5** AFM images of the AZO thin films deposited onto (a) glass, (b) PET, and (c) Si substrate

where $A_n$, $B_n$, and $C_n$ are the Cauchy model parameters. Mean thickness values of the deposited films were found as, 50 nm for glass wafer, 20 nm for PET wafer and 30 nm for Si wafer, respectively.

The differences in the thickness have been formed due to different distances between samples and anode crucible. As can be seen in figure refractive indices of the samples slightly decrease with the increasing wavelength for PET and Si unlike the glass substrate. Tauc plot was used to obtain optical band gap of the AZO thin film for glass and PET substrate. Tauc plot is a simple technique to determine the band gap of the thin films [30]. The method is simply based on a linear extrapolation of the energy axis that gives band gap energy. The absorption coefficient is related to photon energy by the known equation as:

$$\alpha h\nu = \beta(h\nu - E_g)^m \tag{5}$$

where β is constant, alpha represents the absorption coefficient, h is the Planck constant, $\nu$ represents the incident photon frequency, and $E_g$ represents the optical band gap of the semiconductor material. Here $m$, selected as 2, which corresponds to direct allowed transitions. In order to prove calculated optical band gap value photoluminescence measurement was taken using PerkinElmer LS 45 device. The obtained results were indicated in Fig. 5. The optical band gaps of the thin films were determined as 3.48 eV and 3.5 eV for thin films onto glass and PET substrates, respectively. The band gap of the un-doped ZnO thin film is 3.30 eV. When Al doped the ZnO material, the band gap value shift towards to the higher energy value. The obtained band gap values are good harmony with the value determined from the optical method and literature.

Raman spectroscopy measurement was taken place in order to support XRD results. The obtained results are shown in Fig. 6. ZnO, $Al_2O_3$ and substrate peaks, which are PET and Si, were found in Raman spectra [31–35]. The results are also compatible with XRD measurement.

## 4 Conclusion

In this paper, the Al doped ZnO thin films successfully grown on glass, PET and Si substrates via thermionic vacuum arc deposition technique. According to XRD pattern, all films are in polycrystalline form. The one should be noted that bigger crystallite sizes (~ 100 nm) were calculated on Si substrate and lower sizes (~ 20 nm) were calculated on glass substrate. Results are also in accordance with FESEM images. The chosen substrate plays a crucial role during the formation of the crystallites. According to the optical results, average transmittance values of the films defined as 50% and 30% on glass and PET substrate in the visible region, respectively. The optical band gaps of the samples were determined
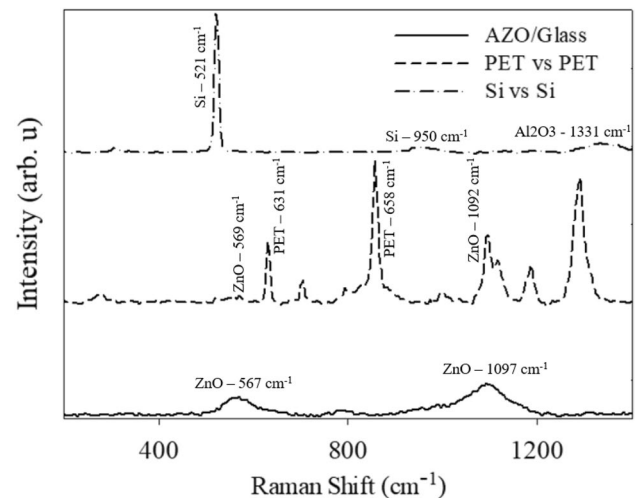


**Fig. 6** Raman spectrum of the AZO thin films deposited onto glass, PET, and Si substrate

as 3.48 eV and 3.5 eV for thin films onto glass and PET substrates, respectively. In Raman analysis, ZnO and $Al_2O_3$ peaks were determined. However, $ZnAl_2O_4$ oxide was not found in Raman spectra. In addition, any impurity such as $NH_3$, water etc. was not detected.

## References

1. V. Srikant, D.R. Clarke, On the optical band gap of zinc oxide. J. Appl. Phys. **83**(10), 5447–5451 (1998)
2. D.C. Look, Recent advances in ZnO materials and devices. Mater. Sci. Eng. **80**(1–3), 383–387 (2001)
3. A. Mitra, R.K. Thareja, V. Ganesan, A. Gupta, P.K. Sahoo, V.N. Kulkarni, Synthesis and characterization of ZnO thin films for UV laser. Appl. Surf. Sci. **174**(3–4), 232–239 (2001)
4. R. Pietruszka, B.S. Witkowski, S. Gieraltowska, P. Caban, L. Wachnicki, E. Zielony, K. Gwozdz, P. Bieganski, E. Placzek-Popko, M. Godlewski, New efficient solar cell structures based on zinc oxide nanorods. Sol. Energy Mater. Sol. Cells **143**, 99–104 (2015)
5. H. Kind, H. Yan, B. Messer, M. Law, P. Yang, Nanowire ultraviolet photodetectors and optical switches. Adv. Mater. **14**(2), 158–160 (2002)
6. A. Tsukazaki, M. Kubota, A. Ohtomo, T. Onuma, K. Ohtani, H. Ohno, M. Kawasaki, Blue light-emitting diode based on ZnO. Jpn. J. Appl. Phys. **44**(5L), L643 (2005)
7. Y. Natsume, H. Sakata, T. Hirayama, H. Yanagida, Low temperature conductivity of ZnO films prepared by chemical vapor deposition. J. Appl. Phys. **72**, 4203 (1992)
8. V. Craciun, J. Elders, J.G.E. Gardeniers, I.W. Boyd, Characteristics of high quality ZnO thin films deposited by pulsed laser deposition. Appl. Phys. Lett. **65**, 2963 (1994)
9. B. Cao, W. Cai, Y. Li, F. Sun, L. Zhang, Ultraviolet-light-emitting ZnO nanosheets prepared by a chemical bath deposition method. Nanotechnology **16**, 1734 (2005)
10. S. Hwangbo, Y.-J. Lee, K.-S. Hwang, Photoluminescence of ZnO layer on commercial glass substrate prepared by sol-gel process. Ceram. Int. **34**, 1237 (2008)

11. S. Pat, R. Mohammadigharehbagh, C. Musaoglu, S. Özen, Ş Korkmaz, Investigation of the surface, morphological and optical properties of boron-doped ZnO thin films deposited by thermionic vacuum arc technique. Mater. Res. Express **5**(6), 066419 (2018)

12. V. Şenay, S. Özen, S. Pat, S. Korkmaz, Some physical properties of a Si-doped nano-crystalline GaAs thin film grown by thermionic vacuum arc, Vaccuum. **119**, 228–232 (2015)

13. Ş. Pat, S. Korkmaz, S. Özen, V. Şenay, Optical, surface and magnetic properties of the Ti-doped GaN nanosheets on glass and PET substrates by thermionic vacuum arc (TVA) method, Part. Sci. Technol. (2018) https://doi.org/10.1080/02726351.2017.1368753

14. R. Vladoiu, C. Porosnicu, A. Mandes, I. Jepu, V. Dinca, A. Marcu, M. Lungu, G. Prodan, L. Avotina, in *Diamond and Carbon Composites and Nanocomposites*, ed. by M. Aliofkhazraei, DLC thin films and carbon nanocomposite growth by thermionic vacuum arc (TVA) technology,(InTech, Rijeka, 2016)

15. R. Ghomri, M.N. Shaikh, M.I. Ahmed, W. Song, W. Cai, M. Bououdina, M. Ghers Pure and (Er, Al) co-doped ZnO nanoparticles: synthesis, characterization, magnetic and photocatalytic properties, J. Mater. Sci. (2018)

16. P.F.H. Inbaraj, J.J. Prince, Optical and structural properties of Mg doped ZnO thin films by chemical bath deposition method, J. Mater. Sci. **29**(2), 935–943 (2018)

17. H. Belaid, M. Nouiri, Z.B. Ayadi, K. Djessas, L. El Mir, Fabrication and electrical properties of Si/PS/ZnO: in solar cell deposited by rf-magnetron sputtering based on nanopowder target material J. Mater. Sci. **26**(11), 8272–8276 (2015)

18. U. Demirkol, S. Pat, R. Mohammadigharehbagh, C. Musaoğlu, M. Özgür, S. Elmas, S. Özen, Ş. Korkmaz, Investigation of the substrate effect for Zr doped ZnO thin film deposition by thermionic vacuum arc technique, J. Mater. Sci. **29**(21), 18098–18104 (2018)

19. G. Musa, H. Ehrich, M. Mausbach, Studies on thermionic cathode anodic vacuum arcs. J. Vacuum Sci. Technol. **12**(5), 2887–2895 (1994)

20. D. Levy, A. Pavese, A. Sani, V. Pischedda, Structure and compressibility of synthetic ZnAl 2 O 4 (gahnite) under high-pressure conditions, from synchrotron X-ray powder diffraction. Phys. Chem. Miner. **28**(9), 612–618 (2001)

21. S. Battiston, C. Rigo, E.D.C. Severo, M.A. Mazutti, R.C. Kuhn, A. Gündel, E.L. Foletto, Synthesis of zinc aluminate ($ZnAl_2O_4$) spinel and its application as photocatalyst. Mater. Res. **17**(3), 734–738 (2014)

22. L. Smrcok, M. Halvarsson, V. Langer, S. Ruppi, A new rietveld refinement of kappa-($Al_2 O_3$). Zeitschrift fuer Kristallographie **216**, 409–412 (2001)

23. J. Kim-Zajonz, High pressure single crystal X-ray diffraction study on ruby. Z. Kristallogr. **214**, 331–336 (1999)

24. K. Lejaeghere, V. Van Speybroeck, G. Van Oost, S. Cottenier, Error estimates for solid-state density-functional theory predictions: an overview by means of the ground-state elemental crystals. Crit. Rev. Solid State Mater. Sci. **39**(1), 1–24 (2014)

25. K. Kihara, G. Donnay, Anharmonic thermal vibrations in ZnO. Can. Mineral. **23**(4), 647–654 (1985)

26. H. Ahsbahs, H. Sowa, High pressure X ray investigation of zincite ZnO single crystals using diamond anvils with an improved shape. J. Appl. Crystallogr. **39**(2), 169–175 (2006)

27. J.L. Hazemann, J.F. Berar, A. Manceau, Rietveld studies of the aluminium-iron substitution in synthetic goethite in Mater. Sci. Forum, **79**, pp. 821–826 (1991)

28. P. Scherrer, Bestimmung der inneren Struktur und der Größe von Kolloidteilchen mittels Röntgenstrahlen. Kolloidchemie Ein Lehrbuch (Springer, Berlin, 1912) (pp. 387–409)

29. A. Patterson, The Scherrer formula for x-ray particle size determination. Phys. Rev. **56**(10), 978–982 (1939)

30. J. Tauc, Optical properties and electronic structure of amorphous Ge and Si, Mater. Res. Bull. **3**(1), 37–46 (1968)

31. M.S. Jang, M.K. Ryu, M.H. Yoon, S.H. Lee, H.K. Kim, A. Onodera, S. Kojima, A study on the Raman spectra of Al-doped and Ga-doped ZnO ceramics. Curr. Appl. Phys. **9**(3), 651–657 (2009)

32. M.F. Cerqueira, T. Viseu, J. Ayres de Campos, A.G. Rolo, T. de Lacerda-Aroso, F. Oliveira, I. Bogdanovic-Radovic, E. Alves, M.I. Vasilevskiy, Raman study of insulating and conductive ZnO:(Al, Mn) thin films. phys. status solidi (A) **212**(10), 2345–2354 (2015)

33. P. Fang, M. He, Y.L. Xie, M.F. Luo, XRD and raman spectroscopic comparative study on phase transformation of gamma-Al2O3 at high temperature, Guang pu xue yu guang pu fen xi, 26(11), 2039–2042 (2006)

34. N. Tong, C.J. Zhu, L.X. Song, C.H. Zhang, G.Q. Zhang, Y.X. Zhang, Characteristics of raman spectra of polyethylene terephthalate, Guang pu xue yu guang pu fen xi, 36(1), 114–118 (2016)

35. X.S. Zhao, Y.R. Ge, J. Schroeder, P.D. Persans, Carrier-induced strain effect in Si and GaAs nanocrystals. Appl. Phys. Lett. **65**(16), 2033–2035 (1994)